Properties of defect modes in periodic lossy multilayer with negative index materials

A. Aghajamali [1,2*] and M. Barati [2†]

[1] *Young Researchers Club,*
Science and Research Branch,
Islamic Azad University, Fars, Iran

[2] *Department of Physics,*
Science and Research Branch,
Islamic Azad University, Fars, Iran

Abstract

Transmission properties of one-dimensional lossy photonic crystals composed of negative and positive refractive index layers with one lossless defect layer at the center of the crystal are investigated by the characteristic matrix method. The results show that as the refractive index and thickness of the defect layer increase the frequency of the defect mode decreases. In addition, it is shown that the frequency of the defect mode is sensitive to the incidence angle, polarization and physical properties of the defect layer but it is insensitive to the small lattice loss factor. The height of the defect mode is very sensitive to the loss factor, incidence angle, polarization, refractive index and thickness of the defect layer. It was also shown that the height and the width of the defect mode are affected by the number of the lattice period and the loss factor. The results can lead to designing new types of narrow filter structures and other optical devices.

* email address: alireza.aghajamali@fsriau.ac.ir
† email address: barati@susc.ac.ir

I. INTRODUCTION

Photonic crystals (PCs) were first introduced theoretically by Yablonovitch [1]., and experimentally by John [2]. PCs, constructed with periodic structure of artificial dielectrics or metallic materials, have attracted many researchers in the past two decades for their unique electromagnetic properties and scientific and engineering applications [1–6]. These crystals indicate a range of forbidden frequencies, called photonic band gap, as a result of Bragg scattering of the electromagnetic waves passing through such a periodical structure [7, 8]. As the periodicity of the structure is broken by introducing a layer with different optical properties, a localized defect mode will appear inside the band gap. Enormous potential applications of PCs with defect layers in different areas, such as light emitting diodes, filters and fabrication of lasers have made such structures are interesting research topic in this field.

Negative index materials (NIMs) with simultaneously negative permittivity and permeability, known as left-handed materials or metamaterials, were introduced by Veselago [9] nearly forty years ago. After the experimental realization of metamaterials by Smith et al. [10], such materials have received attention for their very unusual electromagnetic properties [11–17]. By possibility of manufacturing PCs with metamaterials, called metamaterial photonic crystals (MPCs) in recent years, a new research area was opened to researchers where numerous interesting results have been reported so far. Among the papers published in MPCs properties, there are a number of reports in such structures with defect layers. The properties of the defect modes in different one-dimensional (1D) conventional PC and 1D MPC have been reported by several authors [18–34].

In this paper the characteristic matrix method is used to investigate the effects of the lossless negative and positive defect layers on the defect modes in 1D lossy MPC transmission spectra. The paper is organized as follows: the MPC structure and theoretical formulation (characteristic matrix method) are described in Section 2, the numerical results and discussions are presented in Section 3 and the paper is concluded in Section 4.

II. MPC STRUCTURE AND CHARACTERISTIC MATRIX METHOD

A schematic diagram of a one-dimensional MPC structure with defect layer is shown in figure 1. The MPC structure is composed of alternative NIM layers (layers A) and PIM layers (layers B), where NIM is dispersive and dissipative. The thickness and the refractive index of the layers are d_A and d_B, n_A and n_B, respectively. Layer C is a defect layer and is assumed to be a lossless

and non dispersive material with thickness and refractive index of d_C and n_C, respectively. The calculations are performed using the characteristic matrix method [34], which is the most effective technique to analyze the transmission properties of PCs. The characteristic matrix of the structure is given by:

$M[d] = (M_A M_B)^{N/2} M_C (M_B M_A)^{N/2}$

where M_A, M_B and M_C are the characteristic matrices of layers A, B, and C. The characteristic matrix M_i for TE waves at incidence angle θ_0 in vacuum is given by

$$M_i = \begin{bmatrix} \cos\gamma_i & \frac{-i}{p_i}\ \sin\gamma_i \\ -i\ p_i\ \sin\gamma_i & \cos\gamma_i \end{bmatrix} \tag{1}$$

where $\gamma_i = (\omega/c)\, n_i d_i \cos\theta_i$, c is speed of light in vacuum, θ_i is the angle of refraction inside the layer i with refractive index n_i and $p_i = \sqrt{\varepsilon_i/\mu_i}\ \cos\theta_i$, where $\cos\theta_i = \sqrt{1 - (n_0^2\ \sin^2\theta_0/n_i^2)}$. The refractive index is given as $n_i = \pm\sqrt{\varepsilon_i \mu_i}$ [30, 35], where the positive and negative signs are assigned for the PIM and NIM layers, respectively.

The final characteristic matrix for an N period structure is given by:

$$[M(d)]^N = \prod_{i=1}^{N} M_i \equiv \begin{pmatrix} m_{11} & m_{12} \\ m_{21} & m_{22} \end{pmatrix} \tag{2}$$

where $m_{i,j}(i, j = 1, 2)$ are the matrix elements of $[M(d)]^N$. The transmission coefficient of the multilayer is calculated by:

$$t = \frac{2\ p_0}{(m_{11} + m_{12}\ p_s)\ p_0 + (m_{21} + m_{22}\ p_s)} \tag{3}$$

where $p_0 = n_0\ \cos\theta_0$ and $p_s = n_s\ \cos\theta_s$. The transmissivity of the multilayer is given by

$$T = \frac{p_s}{p_0}|t|^2. \tag{4}$$

The transmissivity of the multilayer for TM waves can be obtained by changing $p_i = \sqrt{\mu_i/\varepsilon_i}\cos\theta_i$, $p_0 = \cos\theta_0/n_0$, and $p_s = \cos\theta_s/n_s$.

The permittivity and permeability of layer A with negative refracting index in the microwave region are complex and are defined as [36],

$$\varepsilon_A(f) = 1 + \frac{5^2}{0.9^2 - f^2 - i\gamma f} + \frac{10^2}{11.5^2 - f^2 - i\gamma f} \tag{5}$$

$$\mu_A(f) = 1 + \frac{3^2}{0.902^2 - f^2 - i\gamma f} \tag{6}$$

where f and γ are the frequency and damping frequency in GHz, respectively. The behaviours of the real parts of the permittivity and permeability of layer A, $\varepsilon_A^{'}$ and $\mu_A^{'}$, versus frequency have been discussed in our previous report [37].

III. NUMERICAL RESULTS AND DISCUSSION

The transmission spectrum of the MPC structure was calculated based on the theoretical model described on the previous section. The calculations are carried out in the region where ε_A' and μ_A' are simultaneously negative, where a new gap, called the zero-$\bar{n}$ gap [36], will appear [36–39]. Layer B is assumed to be the vacuum layer with $\varepsilon_B = \mu_B = 1$. The thickness of layers A and B are chosen as $d_A = 6$mm and $d_B = 12$mm, respectively. The defect layer C is either NIM or PIM non dispersive and non dissipative. The total number of the lattice period is selected to be $N = 16$ [37].

The transmission spectrum for $d_C = 24$mm with positive refractive index of $n_C = 0.75, 1.25, 1.75$ and 2.25, for two different loss factors ($\gamma = 0.2 \times 10^{-3}$ GHz and $\gamma = 8 \times 10^{-3}$ GHz) and for normal incidence are shown in figure 2. As it is clearly seen, the rate of the transmittance and the height of the defect modes are affected by the loss factor. The frequency of the defect modes as a function of the refractive index of the defect PIM and NIM layers for normal incidence and for two different small lattice's loss factors are show in figure 3. As it is seen, the frequency of the defect modes decreases as n_C increases and the modes are nearly insensitive to the small loss factors. In addition, for the PIM defect layer (figure 3(a)) two defect modes appear for some specified refractive indices. The behaviour is quite different in the NIM defect layer (figure 3(b)) where no defect modes are observed in some specific regions.

The effects of n_C on the height of the defect modes for regions I, II and III are shown in figure 3(a) for PIM defect layer and for two different loss factors in figure 4. It is seen that the height of the defect modes almost quadratically depends on the refractive index. The minimum height decreases for the regions with large n_C. Moreover, the height of the modes is very sensitive to the loss factor and decreases as γ increases. The transmission spectrum for $n_C = 1$ and $d_C = 4, 16, 24$ and 32mm and for two different loss factors ($\gamma = 0.2 \times 10^{-3}$ GHz and $\gamma = 8 \times 10^{-3}$ GHz) are presented in figure 5. As it is seen, the frequency of the defect modes move toward the lower frequencies (figure 5(a)) and the height of modes decrease as the thickness of the defect layer increases (figure 5(b)). The behaviors of the frequency and height of the defect modes versus d_C for two different γ are shown in figures 6 and 7, respectively. As it is seen, the frequency of the defect modes is nearly insensitive to the loss factors but the height is very sensitive to γ and decreases as the loss factors increases.

In this section, the effects of the incidence angle on the defect transmission spectra are investigated. The transmission spectra of TE and TM polarized waves for $0°$, $25°$, $50°$ and $75°$ incidence

angles for $d_C = 8$mm, $n_C = 2.5$, and for two different loss factors ($\gamma = 0.2 \times 10^{-3}$ GHz and $\gamma = 8 \times 10^{-3}$ GHz) are shown in figures 8 and 9, respectively.

As it is observed from figure 8, and reported in [37, 39], the width, the depth and the central frequency of the band gap for TE waves increase as the incidence angle increases. But, for TM waves, the gap disappears for the incidence angles greater than $\approx 50°$. As θ_0 increases the width and the depth of gap decrease and the central frequency shifts toward the higher frequencies (figure 9). The behaviour of the defect mode's frequency for TE and TM waves as a function of the incidence angle for two different loss factors are shown in figure 10. Here it is clearly seen that the frequency of the defect mode is nearly insensitive to the small loss factor and it disappears for TM waves for the incidence angle greater than $\approx 50°$. The change of the height of the defect mode for both polarizations as a function of the incidence angle for two different loss factors is shown in figure 11. It is seen that the height of the defect modes decreases for TE polarized waves while it increases for TM polarized waves as the incidence angle increases. It is also seen that the height of the modes are very sensitive to the loss factor for both polarizations.

In the last part the effects of the number of the lattice period, N, and the loss factor on the transmission properties of the defect mode are studied. So far $N = 16$ was assumed. The results are presented in figures 12 and 13 for normal incidence angle. As it is seen from figure 12(a) and as reported in [37], the width of the band gap for $N > 16$ is almost independent of N. However the depth and the height of the defect mode reduce as N increases for $\gamma = 0.2 \times 10^{-3}$ GHz. It is interesting to note that the frequency of the defect mode remains unchanged but the width of the mode decreases as the number of the lattice period increases (figure 12(b)). The transmission spectra of the structure for four different loss factors and for $N = 16$ are shown in figure 13. As it is seen from figure 13(a) the width and the depth of the band gap and the frequency of the defect mode are nearly insensitive to small loss factor but the transmission is affected by γ [37]. Moreover, the height of the defect mode decreases as the loss factor increases (figure 13(b)).

IV. CONCLUSION

In this paper the transmission properties of one-dimensional lossy photonic crystals with negative and positive refractive indices layers and a lossless defect layer at the center of the crystal were investigated by characteristic matrix method. It was shown that by adding a lossless defect layer to a 1D lossy MPC, a localized defect mode appears inside the band gap. The position of the defect mode depends on the physical properties of the defect layer such as the refractive index

and thickness but it is independent of the loss factor. The results show that as the refractive index and thickness of the defect layer increases the frequency of the defect mode decreases. In addition, it was shown that the frequency and the height of the defect mode are sensitive to the incidence angle and polarization. For a PIM defect layer with the refractive index between 4.75 to 6.25, two defect modes appear in a specific range of the transmittance spectrum, while for an NIM defect layer the spectrum is quite different where no defect modes is observed in a certain range of the refractive index ($n_C = -2$ to -3.5). The absence of the defect mode in some specified region is not clear and is the subject of our future studies. It was also seen that: *i*) by increasing the incidence angle the frequency of the defect mode increases. *ii*) by increasing the thickness of the defect layer the frequency of the defect mode moves toward lower frequencies. *iii*) the height of the defect modes is very sensitive to the loss factors. *iv*) the depth of the band gap increases and consequently the height and the width of the defect mode decrease, so the mode becomes narrower for $N > 16$. *v*) the width and the depth of the band gap and the frequency of the defect modes are nearly insensitive to small loss factors but the height of the defect mode is very sensitive to small γ and decreases as the loss factor increases. Such properties are quite useful in designing new types of optical devices in microwave engineering.

References

[1] Yablonovitch, E., "Inhibited spontaneous emission in solid-state physics and electronics," *Phys. Rev. Lett.*, Vol. 58, 2059-2062, 1987.

[2] John, S., "Strong localization of photons in certain disordered dielectric superlattices," *Phys. Rev. Lett.*, Vol. 58, 2486-2489, 1987.

[3] Noda, S., A. Chutinan, and M. Imada, "Trapping and emission of photons by a single defect in a photonic bandgap structure," *Nature*, Vol. 407, 608-610, 2000.

[4] Massaoudi, S., A. de Lustrac, and I. Huynen, "Properties of metallic photonic band gap material with defect at microwave frequencies: calculation and experimental verification," *J. Electromagn. Waves Appl.*, Vol. 14, 1967-1980, 2006.

[5] Mandal, B. and A. R. Chowdhury, "Spatial soliton scattering in a quasi phase matched quadratic media in presence of cubic nonlinearity," *J. Electromagn. Waves Appl.*, Vol. 1, 123-135, 2007.

[6] Zheng, Q. R., B. Q. Lin, and N. C. Yuan, "Characteristics and applications of a novel compact spiral electromagnetic band-gap (EBG) structure," *J. Electromagn. Waves Appl.*, Vol. 2, 199-213, 2007.

[7] Yablonovitch, E., "Photonic band structure: the face-centered-cubic case employing nonspherical atoms," *Phys. Rev. Lett.*, Vol. 67, 2295-2298, 1991.

[8] Joannopoulos, J. D., S. G. Johnson, J. N. Winn, and R. D. Meada, *Photonic crystals: Modeling the flow of light*, Princeton University Press, Princeton, 2008.

[9] Veselago, V. G., "The electrodynamics of substances with simultaneously negative values of ε and μ," *Sov. Phys. Usp.*, Vol. 10, 509-514, 1968.

[10] Smith, D. R., W. J. Padilla, D. C. Vier, S. C. Nemat-Naser, and S. Schuitz, "Composite medium with simultaneously negative permeability and permittivity," *Phys. Rev. Lett.*, Vol. 84, 4184-4187, 2000.

[11] Engheta, N. and R. W. Ziolkowski, *Metamaterials: Physics and engineering explorations*, John Wiley & Sons, New Jersey, 2006.

[12] Caloz, C. and T. Itoh, *Electromagnetic metamaterials: Transmission line theory and microwave applications*, John Wiley & Sons, New Jersey, 2006.

[13] Cai, W. and V. Shalaev, *Optical metamaterials: Fundamentals and applications*, Springer, New York, 2010.

[14] Eleftheriades, G. V. and K. G. Balmain, *Negative refraction metamaterials: Fundamentals properties and applications*, John Wiley & Sons, New Jersey, 2005.

[15] Novitsky, A. V. and L. M. Barkovsky, "Guided modes in negative-refractive-index fibres," *J. Opt. A Pure Appl. Opt.*, Vol. 7, S51-S56, 2005.

[16] Cory, H. and T. Blum, "Surface-wave propagation along a metamaterial cylindrical guide," *Microw. Opt. Technol. Lett.*, Vol. 44, 31-35, 2005.

[17] Kim, K. Y., J. H. Lee, Y. K. Cho, and H. S. Tae, "Electromagnetic wave propagation through doubly dispersive subwavelength metamaterial hole," *Opt. Express*, Vol. 13, 3653-3665, 2005.

[18] Lotfi, E., K. Jamshidi-Ghaleh, F. Moslem, and H. Masalehdan, "Comparison of photonic crystal narrow filters with metamaterials and dielectric defects," *Eur. Phys. J. D*, Vol. 60, 369-372, 2010.

[19] Zhu, Q. and Y. Zhang, "Defect modes and wavelength tuning of one-dimensional photonic crystal with lithium niobate," *Optik*, Vol. 120, 195-198, 2009.

[20] Abdel-Rahman, E. and A. Shaarawi, "Defect mode in periodic and quasiperiodic one-dimensional photonic structures," *J Mater Sci: Mater Electron*, Vol. 20, S153-S158, 2009.

[21] Ansari, N., M. M. Tehranchi, and M. Ghanaatshoar, "Characterization of defect modes in one-dimensional photonic crystals: An analytic approach," *Physica B*, Vol. 404, 1181-1186, 2009.

[22] Li, X., K. Xie, and H. M. Jiang, "Properties of defect modes in one-dimensional photonic crystals containing two nonlinear defects," *Opt. Commun.*, Vol. 282, 4292-4295, 2009.

[23] Wu, C. -J. and Z. H. Wang, "Properties of defect modes in one-dimensional photonic crystals," *Progress In Electromagnetics Research*, Vol. 103, 169-184, 2010.

[24] Ansari, N. and M. M. Tehranchi, "Influence of filling fraction on the defect mode and gap closing of a one-dimensional photonic crystal: An analytical approach," *Physica B*, Vol. 405, 2900-2906, 2010.

[25] Gharaati, A. and H. Azarshab, "Characterization of defect modes in one-dimensional ternary metallo-dielectric nanolayered photonic crystal," *Progress In Electromagnetics Research B*, Vol. 37, 125-141, 2012.

[26] Zhang, W., P. Han, A. Lan, Y. Li, and X. Zhang, "Defect modes tuning of one-dimensional photonic crystals with lithium niobate and silver material defect," *Physica E*, Vol. 44, 813-815, 2012.

[27] Aly, A. H. and H. A. Elsayed, "Defect mode properties in a one-dimensional photonic crystal," *Physica B*, Vol. 407, 120-125, 2012.

[28] Chen, Y. H., G. Q. Liang, J. W. Dong, and H. Z. Wang, "Derivation and characterization of dispersion of defect modes in photonic band gap from stacks of positive and negative index materials," *Phys. Lett. A*, Vol. 351, 446-451, 2006.

[29] Kang-Song, T., X. Yuan-Jiang, and W. Shuang-Chun, "Defect in photonic crystal with negative index material," *Optoelectron. Lett.*, Vol. 2, 118-121, 2006.

[30] Jiang, H., H. Chen, H. Li, and Y. Zhang, "Omnidirectional gap and defect mode of one-dimensional photonic crystals containing negative-index materials," *Appl. Phys. Lett.*, Vol. 83, 5386-5388, 2003.

[31] Wang, L. G., H. Chen, and S. Y. Zhu, "Omnidirectional gap and defect mode of one-dimensional photonic crystals with single-negative materials," *Phys. Rev. B*, Vol. 70, 245102-245107, 2004.

[32] Xu, Q., K. Xie, H. Yang, and J. Tang, "Periodic defect modes of one-dimensional crystals containing single-negative materials," *Optik*, Vol. 121, 1558-1562, 2010.

[33] Xiang, Y., X. Dai, S. Wen, and D. Fan, "Properties of omnidirectional gap and defect mode of one-dimensional photonic crystal containing indefinite metamaterials with a hyperbolic dispersion," *J. Appl. Phys.*, Vol. 102, 093107-093111, 2007.

[34] Born, M. and E. Wolf, *Principles of Optics: Electromagnetic theory of propagation, Interference and diffraction of light*, Cambridge University Press, UK, 2005.

[35] Zhang, L., Y. Zhang, L. He, Z. Wang, H. Li, and H. Chen, "Zero-$\bar{n}$ gaps of photonic crystals consisting of positive and negative index materials in microstrip transmission lines," *J. Phys. D: Appl. Phys.*, Vol. 40, 2579-2587, 2007.

[36] Li, J., L. Zhou, C. T. Chan, and P. Sheng, "Photonic band gap from a stack of positive and negative index materials," *Phys. Rev. Lett.*, Vol. 90, 083901-083904, 2003.

[37] Aghajamali, A. and M. Barati, "Effects of normal and oblique incidence on zero-$\bar{n}$ gap in periodic lossy multilayer containing double-negative materials," *Physica B*, Vol. 407, 1287-1291, 2012.

[38] Daninthe, H., S. Foteinopoulou, C. M. Soukoulis, "Omni-reflectance and enhanced resonant tunneling from multilayers containing left-handed materials," *Photoni. Nanostruct.*, Vol. 4, 123-131, 2006.

[39] Awasthi, S. K., A. Mishra, U. Malaviya, and S. P. Ojha, "Wave propagation in a one-dimensional photonic crystal with metamaterial," *Solid State Commun.*, Vol. 149, 1379-1383, 2009.

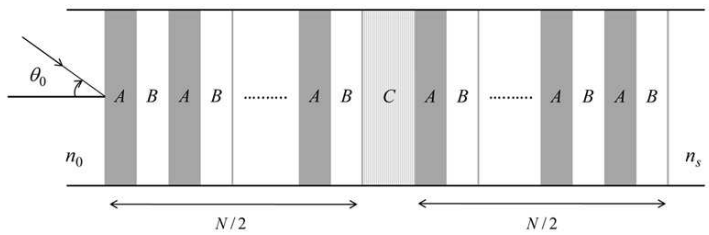

FIG. 1: Schematic of 1D MPC structure with a defect layer. Layer A is NIM and layer B is PIM materials. N is the number of lattice period and θ_0 is the incidence angle.

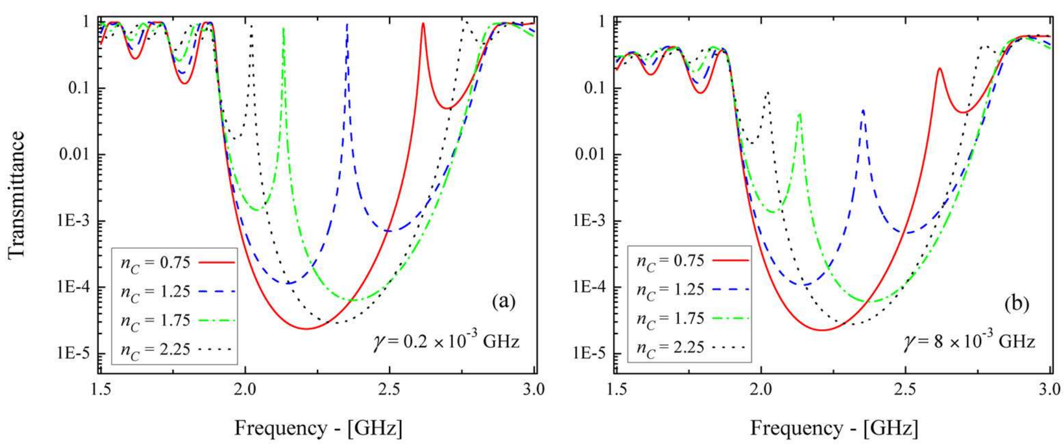

FIG. 2: Transmission spectra of 1D MPC structure at normal incidence for different positive refractive indices of the lossless defect layer, with $d_C = 24$mm and for two different lattice loss factors (a) $\gamma = 0.2 \times 10^{-3}$ GHz (b) $\gamma = 8 \times 10^{-3}$ GHz.

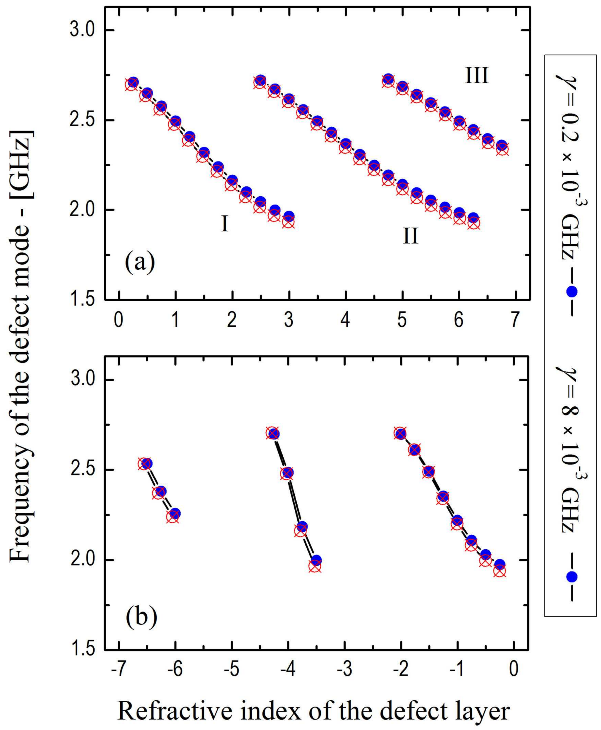

FIG. 3: Dependence of the defect mode frequency on the (a) positive and (b) negative refractive index of the lossless defect layer (n_C) for two different lattice loss factors ($\gamma = 0.2 \times 10^{-3}$ GHz and $\gamma = 8 \times 10^{-3}$ GHz).

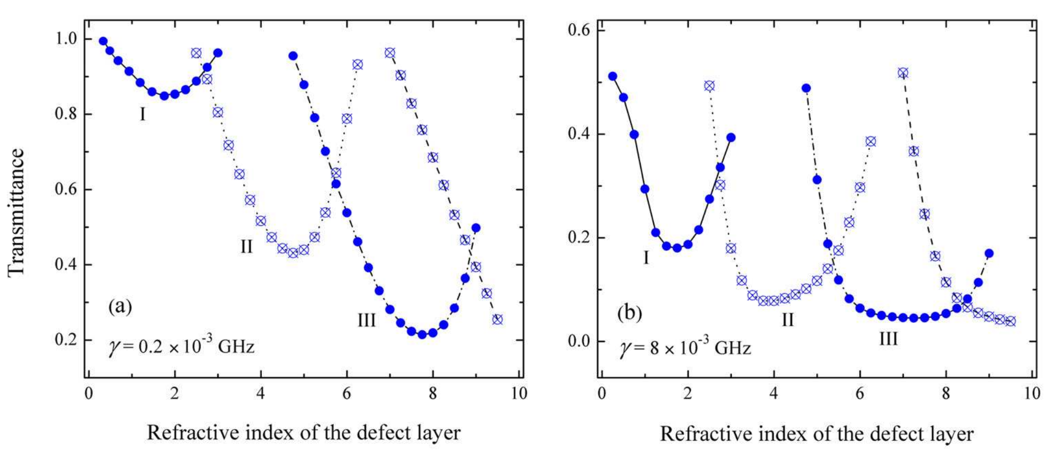

FIG. 4: Height of the defect modes versus the positive refractive index of the defect layer, with $d_C = 24$mm and for two different lattice loss factors (a) $\gamma = 0.2 \times 10^{-3}$ GHz (b) $\gamma = 8 \times 10^{-3}$ GHz.

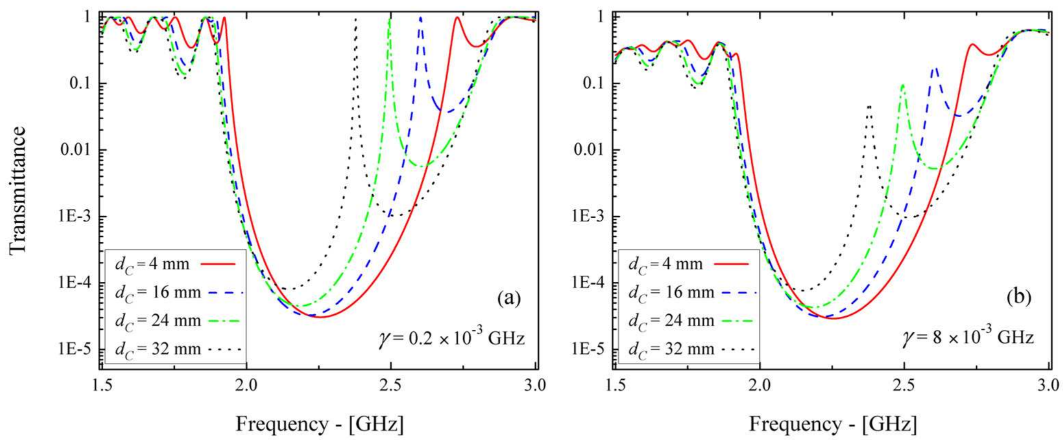

FIG. 5: Transmission spectra of 1D MPC structure at normal incidence, for different thicknesses of the lossless defect layer, and for two different lattice's loss factors (a) $\gamma = 0.2 \times 10^{-3}$ GHz (b) $\gamma = 8 \times 10^{-3}$ GHz for with $n_C = 1$.

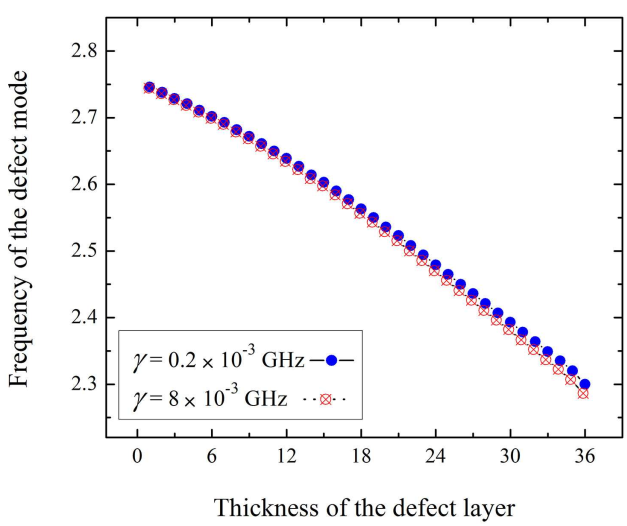

FIG. 6: Dependence of the defect mode frequency on the thickness of the defect layer for two different lattice loss factors for $n_C = 1$.

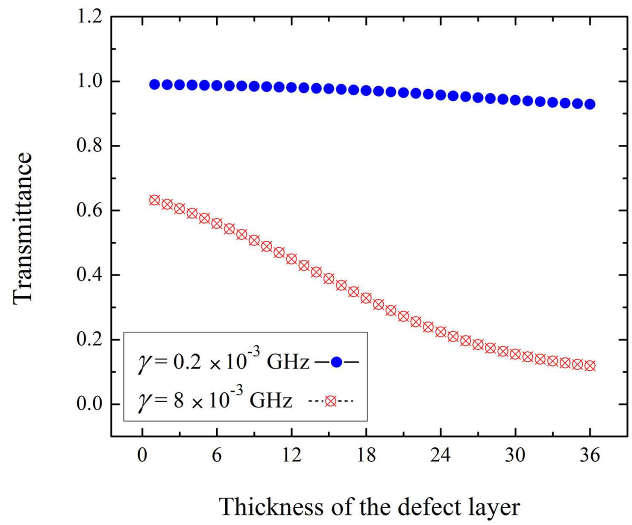

FIG. 7: Height of the defect mode versus thickness of the defect layer for two different lattice loss factors, for $n_C = 1$.

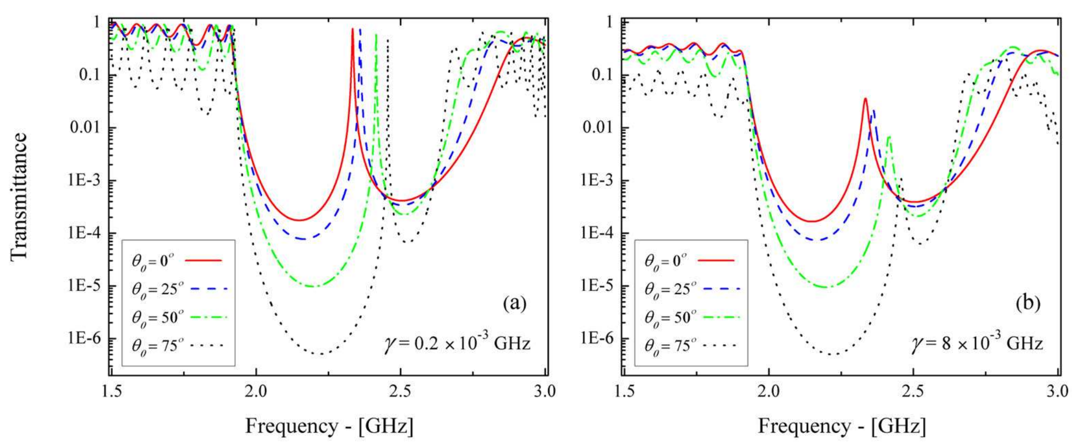

FIG. 8: TE polarized wave transmission spectra of 1D MPC structure, for different incidence angles with $n_C = 2.5$ and $d_C = 8$mm and for two different lattice loss factors (a) $\gamma = 0.2 \times 10^{-3}$ GHz (b) $\gamma = 8 \times 10^{-3}$ GHz.

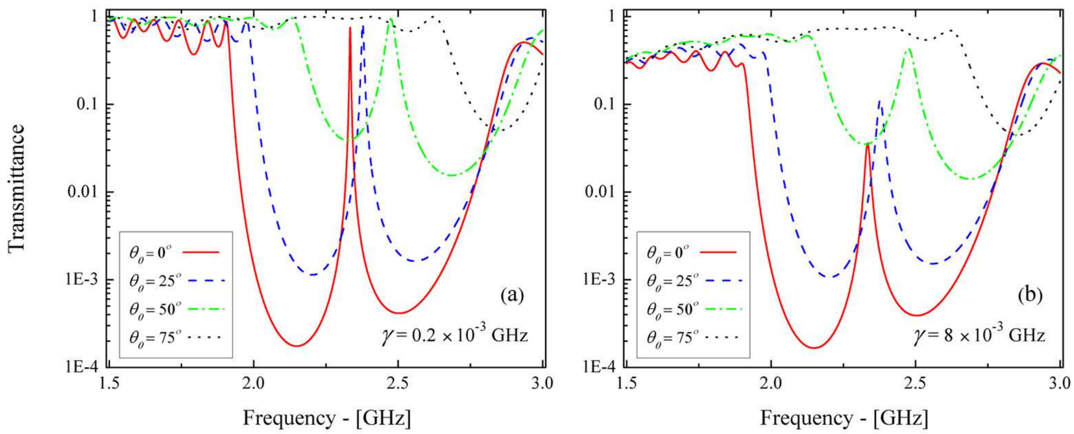

FIG. 9: The same as figure 8 but for TM polarized wave.

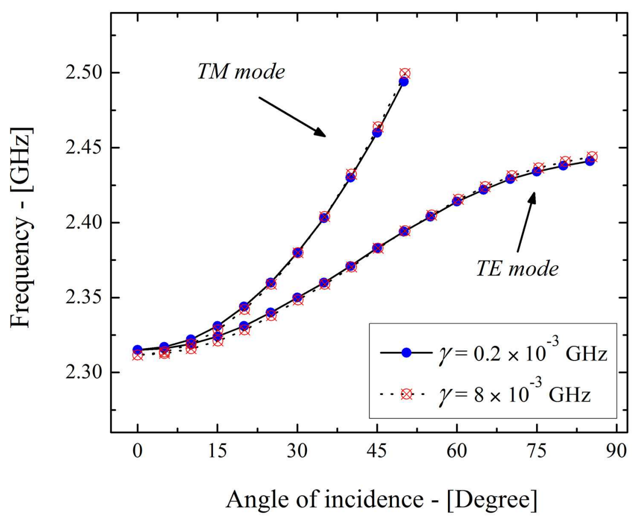

FIG. 10: Frequency of the defect mode as a function of incidence angle for both polarizations and for two different lattice loss factors.

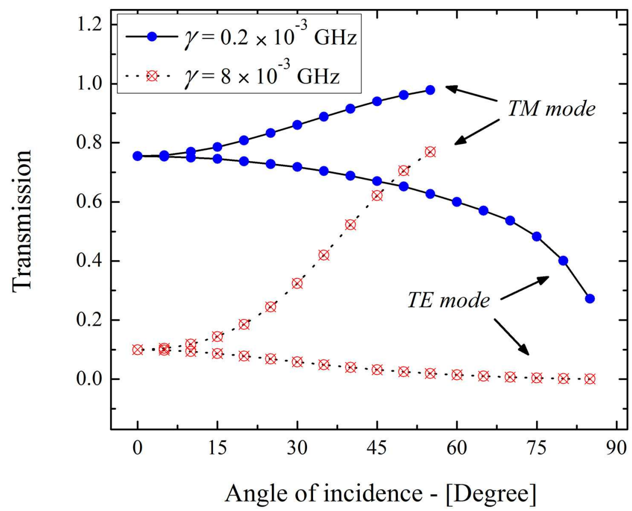

FIG. 11: Height of defect mode as a function of incidence angle for both polarizations and for two different lattice loss factors.

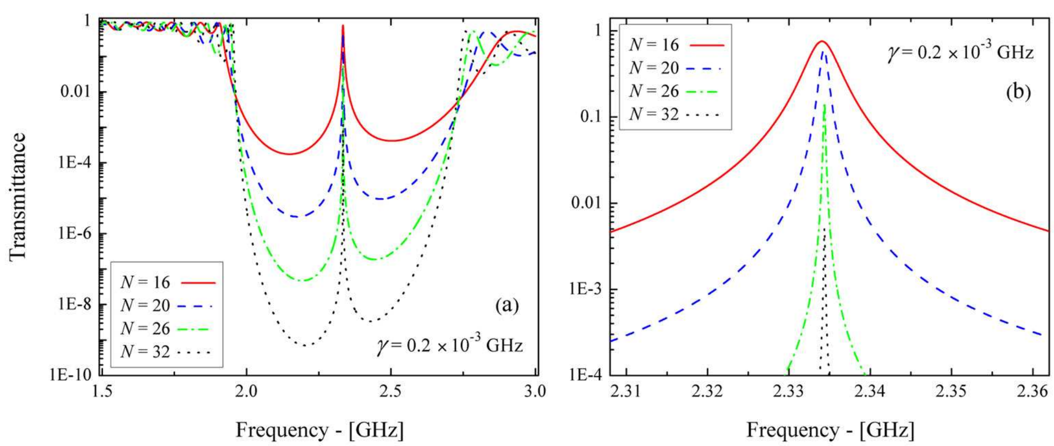

FIG. 12: Transmission spectra of 1D MPC structure at normal incidence, for different number of the lattice period and for $\gamma = 0.2 \times 10^{-3}$ GHz.

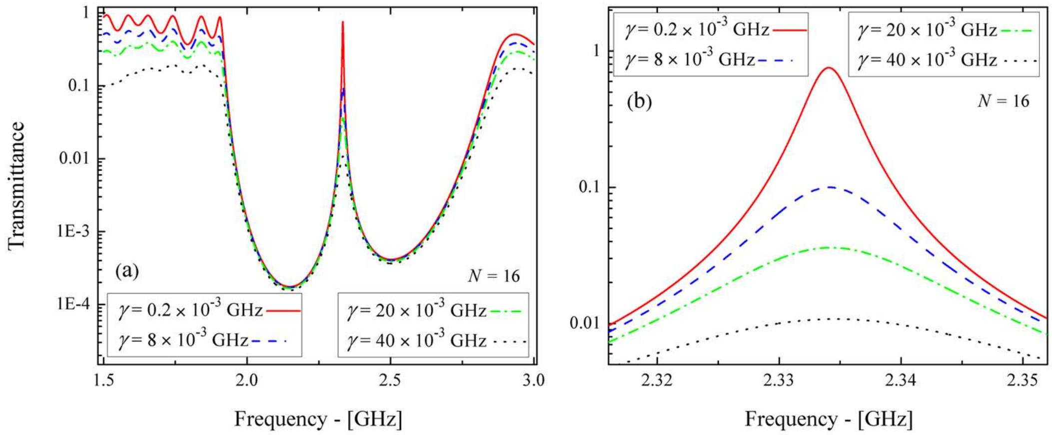

FIG. 13: Transmission spectra of 1D MPC structure at normal incidence, for different lattice loss factors for $N = 16$.